

Response of Solid ^4He to External Stress: Interdigital Capacitor Solid Level Detector and Optical Interferometer

J. Fay, Y. Wada*, R. Masutomi, T. Elkholy and H. Kojima

Serin Physics Laboratory
Rutgers University
Piscataway, New Jersey 08854

abstract

Two experiments are being conducted to observe the liquid/solid interface of ^4He near 1 K. Interesting instabilities are expected to occur when the solid is non-hydrostatically stressed. (1) A compact interdigital capacitor is used as a level detector to observe solid ^4He to which stresses are applied externally. The capacitor consists of 38 interlaced $50\ \mu\text{m}$ wide and $3.8\ \text{mm}$ long gold films separated by $50\ \mu\text{m}$ and deposited onto a $5\ \text{mm}$ by $5\ \text{mm}$ sapphire substrate. The capacitor is placed on one flat end wall of a cylindrical chamber ($xx\ \text{mm}$ diameter and $xx\ \text{mm}$ long). The solid is grown to a known height and a stress is applied by a tubular PZT along the cylindrical axis. The observed small change in height of the solid at the wall is linearly proportional to the applied stress. The solid height decreases under compressive stress but does not change under tensile stress. The response of the solid on compressive stress is consistent with the expected quadratic dependence on strain. (2) Interferometric techniques are being developed for observing the solid ^4He surface profile. A laser light source is brought into the low temperature region via single mode optical fiber. The interference pattern is transmitted back out of the low temperature apparatus via optical fiber bundle. The solid ^4He growth chamber will be equipped with two PZT's such that stress can be applied from orthogonal directions. Orthogonally applied stress is expected to induce surface instability with island-like deformation on a grid pattern. Apparatus design and progress of its construction are described.

I. Motivation

Stress-driven instability or Grinfeld instability(GI)[1] arises from a general phenomenon of nature that a non-hydrostatically stressed solid can decrease elastic energy by rearrangement of their material particles in the vicinity of the phase boundary by processes such as melting-freezing, evaporation-sublimation and surface diffusion. GI is intimately related to phenomena of practical importance such as pattern formation in epitaxial crystal growth, surface reaction rate on pre-stressed solids, surface cracking and corrosion. Quantum crystals of ^4He provide an excellent testing ground for GI effects. For investigation of interface related phenomena, the solid/liquid interface of ^4He below 2 K has many advantages such as small latent heat, rapid melting and freezing and superfluid heat conduction. The ultimate goal of our research is to study the instability of solid surface morphology under externally applied stresses. Stripe and island patterns are expected to form at the interface under uniaxially applied stress and orthogonally applied stress, respectively.

The GI sets in only beyond a certain threshold stress. If the applied stress does not exceed the threshold value, ^4He solid/liquid interface reacts to the stress by lowering its height. A simple interdigital capacitor solid height detector is being developed to check this effect. For observing the interfacial pattern, an optical interferometer is being built using optical fiber technology. Progress in both of these studies is presented in this report.

II. Simplified Explanation of Grinfeld Instability

Imagine that a cubic solid body is divided up into cells as shown in Fig. 1a. In equilibrium and with no external forces applied onto the solid, the cells are all identical small cubes. When an external force is applied on the vertical faces along x-axis as shown in Figure 1c, each cell stretches along x-axis. Work is done on the solid and the elastic energy of the solid increases by an amount E_{reg} . Now, let's imagine that one cell in Figure 1c, by fluctuation, moves up onto the originally horizontal surface and makes a "bump" and a "hole" as shown in Figure 1e. If the elastic energy is to be maintained constant, the shape of the bump and the hole must keep the same shape as before moving. And for the bump to keep its shape, the same forces per unit area along the horizontal direction must be maintained

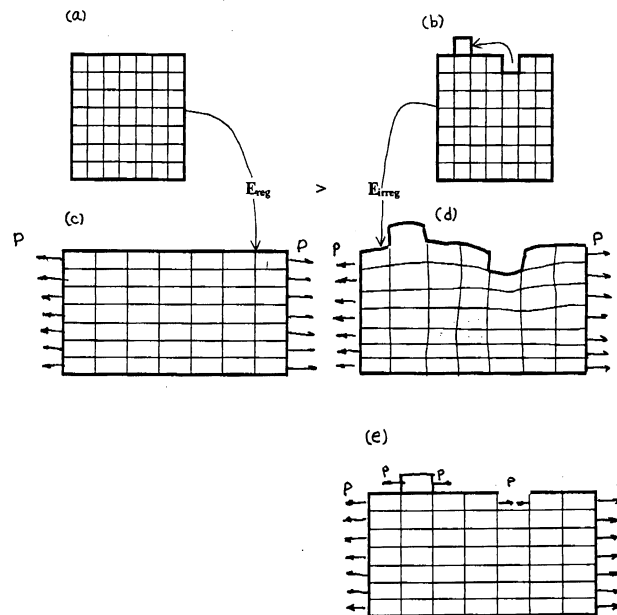


Figure 1

along the x-axis. Then, the elastic energy of the solid in Fig. 1c and Fig. 1e would be the same. Note, however, that there are no direct external horizontal forces acting neither on the bump nor on the sides of the hole. In the absence of the external forces to maintain the original shape, the bump and the hole proceed to “relax” towards a shape such as shown in Fig. 1d. The relaxation proceeds because the elastic energy is reduced in the process. The net increase of the elastic energy of the body in Fig. 1d, E_{irreg} , is less than E_{reg} . Thus the shape in Fig. 1d is more favorable than that in Fig. 1c. This is the physical origin of Grinfeld Instability.[2]

The first qualitative observations of GI are thought to be made by Bodensohn et al[3] on a rapidly cooled helium-4 crystals. More systematic measurements with externally controlled stress were carried out later by Torii and Balibar[4] who demonstrated the appearance of surface corrugation beyond a certain threshold stress.

III. Apparatus and Preliminary Results

1. Interdigital Capacitor Level Detector and Solid Growth Chamber

Consider a rectangularly shaped slab of solid ^4He at its melting pressure at low temperature in equilibrium with superfluid liquid phase. Imagine that a uniaxial stress is applied on the solid. To maintain equilibrium, the chemical potentials of the solid and liquid must remain equal. Thus, the solid melts and the interface lowers by ΔH . If solid ^4He can be considered isotropic[5], ΔH is given by[4,6]:

$$\Delta H = \frac{(1-\nu)\delta^2}{2Y^2 g(r_c - r_L)}. \quad \text{Eq. 1}$$

Here, δ is the applied strain on the solid, $\tilde{n}_C = 0.1908 \text{ g/cm}^3$ the density of solid, $\tilde{n}_L = 0.1729 \text{ g/cm}^3$ the density of liquid, and $Y = 3 \times 10^8 \text{ dyne/cm}^2$ the Young’s modulus of solid, $\nu = 1/3$ the Poisson’s ratio, g the acceleration of gravity. The gravitational acceleration constant plays an important role. Note that the change in height is independent of the direction of the applied stress. So the interface height lowers under both tension and compression applied to the solid.

As an important test of understanding, we carried a preliminary study to check the expected change in height of solid ^4He to which a uniaxial stress is externally applied. The apparatus for this study is shown in Figure 2. A

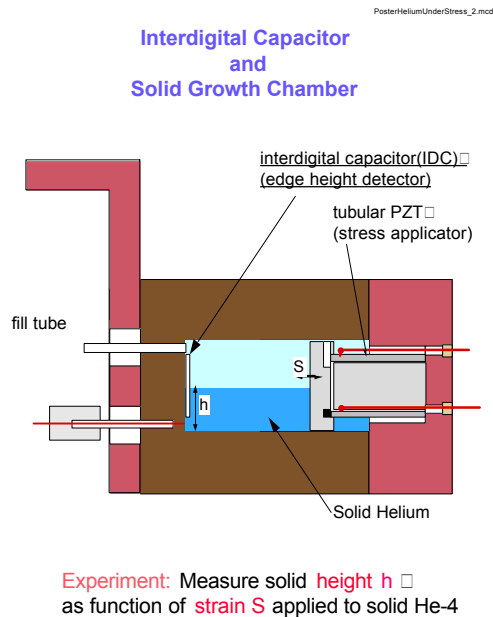


Figure 2

simple interdigital capacitor[7] for detecting the solid height is located at the end of a cylindrical chamber (length $L = 19.8$ mm and diameter = xx mm) in which solid ^4He is grown. Note that the volume of the growth chamber is much greater than our previous one[7]. Measured changes in capacitance directly give the changes in height of the solid at the edge. The minimum detectable change in height is $0.5 \mu\text{m}$ at present. The temperature of the chamber can be lowered to 1.2 K. Smooth growths of solid height can be observed repeatedly as helium is fed into the growth chamber from a gas handling panel at room temperature. Strains are given to the solid by moving the plunger plate attached to a tubular piezoelectric transducer(PZT)[8]. The length of the PZT is varied by the externally applied voltage between the inner and outer electrodes on it.

A typical result at $T = 1.2$ K is shown in Figure 3. The solid was grown to about half way up the growth chamber by slowly feeding in helium. The crystal orientation relative to the growth chamber is not known. The observed change in height is shown in Figure 3 as function of the applied voltage to PZT. The positive applied voltage corresponds to the case of solid under compression. When negative voltages are applied to the solid (now under tension), observed changes are not reproducible and show little change in height.

The applied strain is given by:

$$d = \frac{d_{32}lV_{pzt}}{tL} \quad \text{Eq. 2}$$

where $d_{32} = 0.33 \times 10^{-7}$ mm/V is the piezoelectric constant, $l = 9.5$ mm the length of PZT, $t = 1.0$ mm the thickness of tubular PZT, $L = 19.8$ mm the length of cylinder (and hence solid ^4He) and V_{pzt} the applied voltage to PZT. Substituting Eq. (2) into Eq. (1) gives the expected change in height shown in Figure 3.

As expected, the data indicate lowering of height as compression is applied.

However, it cannot be claimed, particularly in the negative strain side, that the height decreases in proportion to the square of applied strain. The scatter in data is large. The scatter is in part caused by the irreproducible relaxation in height often observed after a change in applied voltage is made. Some stick-slip motion of solid at the interdigital capacitor surface could cause this irreproducibility. The small response for negative voltage indicates that solid detaches from the plunger surface. The plunger is

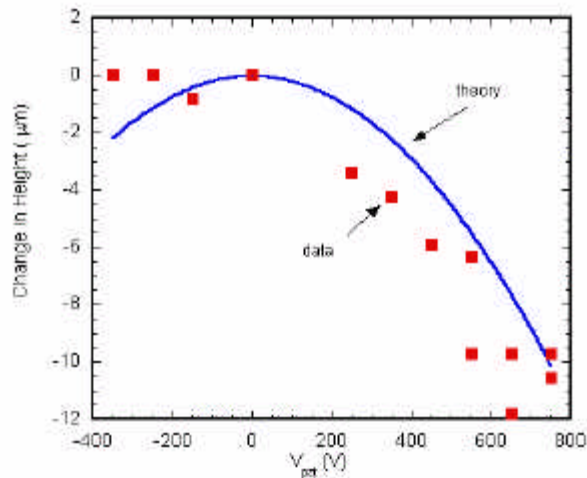


Figure 3

made of machined stycast 1266 which is likely to have roughness of at least $10\ \mu\text{m}$. A glass plate has been used as a plunger surface which also produced results which depend on the direction of strain.[9] Studies are needed to find material and/or surface conditions for pulling on the surface of solid ^4He without detachment.

2. Interferometer Apparatus

August 2003

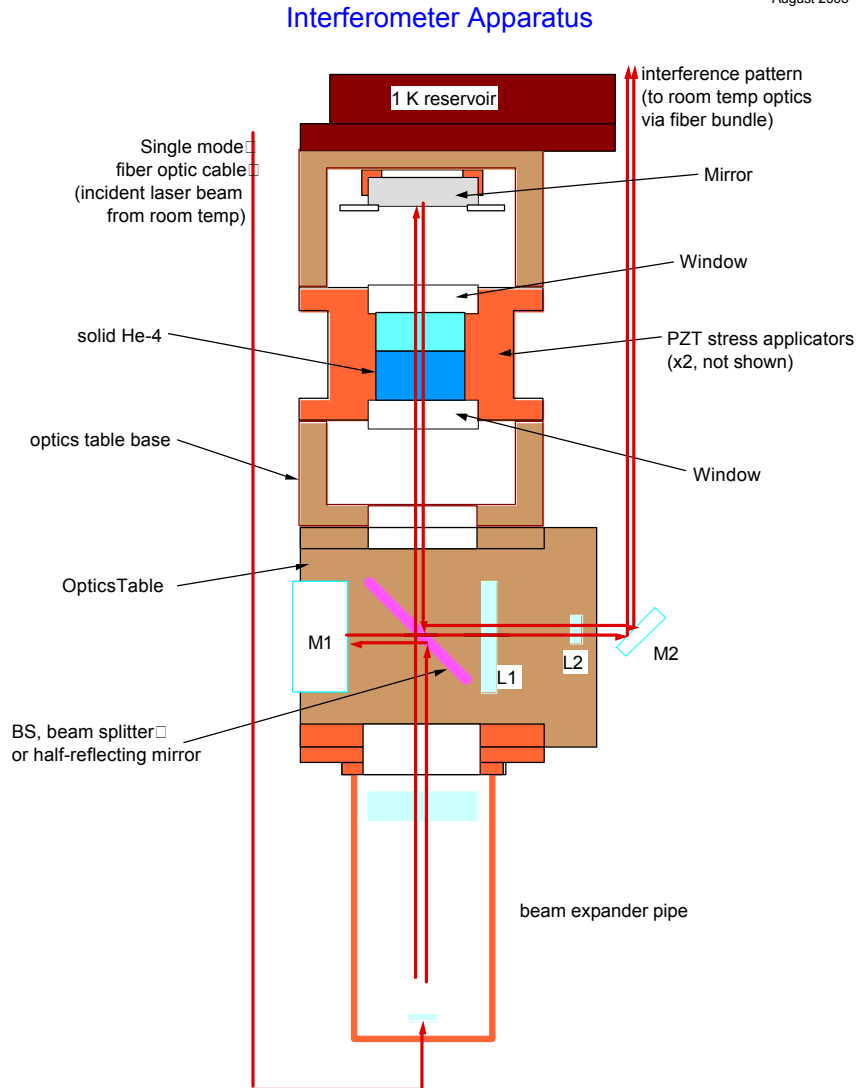


Figure 4

A schematic of the low temperature section of our optical apparatus for directly observing the liquid solid interface is shown in Figure 4. A single mode optical fiber brings the incident He-Ne laser beam down to the beam expander pipe. The expanded beam is split by a beam splitter plate. The reflected beam from the splitter is directed to the mirror M1. The beam reflected from M1 acts as the reference beam. The transmitted beam from the splitter moves up through the solid growth chamber (whose cross section is a $17.8 \times 10.1\ \text{mm}^2$ rectangle and the depth is xx mm) and returns back to the splitter

after reflecting from the upper mirror. The beam interferes with the reference beam and its image is transmitted up into room temperature optics via fiber bundle image conduit (diameter = 3 mm, about 5×10^4 individual fibers).

The image transmitted through the conduit is monitored by a monochrome video camera. A photograph of the low temperature part of the optical system is shown in Figure 5. Pumping on the “1 K reservoir” pot reduces the temperature of the solid growth chamber filled with liquid helium to 1.2 K when the incident laser beam is continuously left on. The reflecting mirror M2 (see Figure 4) is visible in front of the beam splitter holder.

The interference fringe pattern may be analyzed to determine the liquid/solid interface height profile $H(x,y)$. The phase shift from that at some reference position between the two interfering beams may be written as:

$$\Delta f(x, y) = \frac{2p}{\lambda} [\Delta D_B(x, y) + 2(n_s - n_L)\Delta H(x, y)], \quad \text{Eq. 3}$$

where $\Delta D_B(x,y)$ is the “background” path length shift arising from the variation in the distance between M1 and mirror in Figure 4. The difference in indices of refraction of solid and liquid is $(n_s - n_L) = 0.034$. For the wavelength of 630 nm for He-Ne laser, there is one fringe shift per 96 μm of change in height ΔH .

An example of interference pattern is shown in Figure 6. Here, the chamber is cooled to 1.3 K and filled with liquid pressurized to 5 bars. Since there is no solid, the interference pattern is set by the spatial variation in $\Delta D_B(x,y)$. The outline of the chamber is shown by red lines. When the pressure is increased up to the melting pressure, irreproducible initial formation of solid can be seen in the interference pattern near the end of the fill tube. Subsequent to the initial seeding of solid, interference patterns similar to that shown in Figure 7 are often observed. The interference pattern indicates formation of a flat rectangular plateau of solid surface. The spacing of the fringes within the plateau shows that there is a 30 μm difference in height of solid along the long ends of the plateau. Presumably the solid surface height decreases towards the edges of the solid growth chamber. There should be interference pattern corresponding to these sloping surfaces. The expected pattern between the apparent edge of the plateau and the chamber boundary is not visible in the video image probably owing to lack of adequate focusing.

IV. Conclusion

An interdigital capacitor level detector has been developed for observing changes in the height of solid ^4He under uniaxial stress. Preliminary studies show compressive stresses lowers the solid height as expected, but the quadratic dependence on the magnitude of stress is not clearly demonstrated. Tensile stresses do not produce lowering of solid height contrary to expectation. Interferometric observations on solid growth patterns in a rectangular chamber have been made. Solids were formed by feeding helium into the chamber at constant temperature or by cooling at constant pressure. In the first method, a flat solid surface could be observed almost reproducibly. PZTs will be

incorporated in the near future into the chamber for applying external stresses onto the solid.

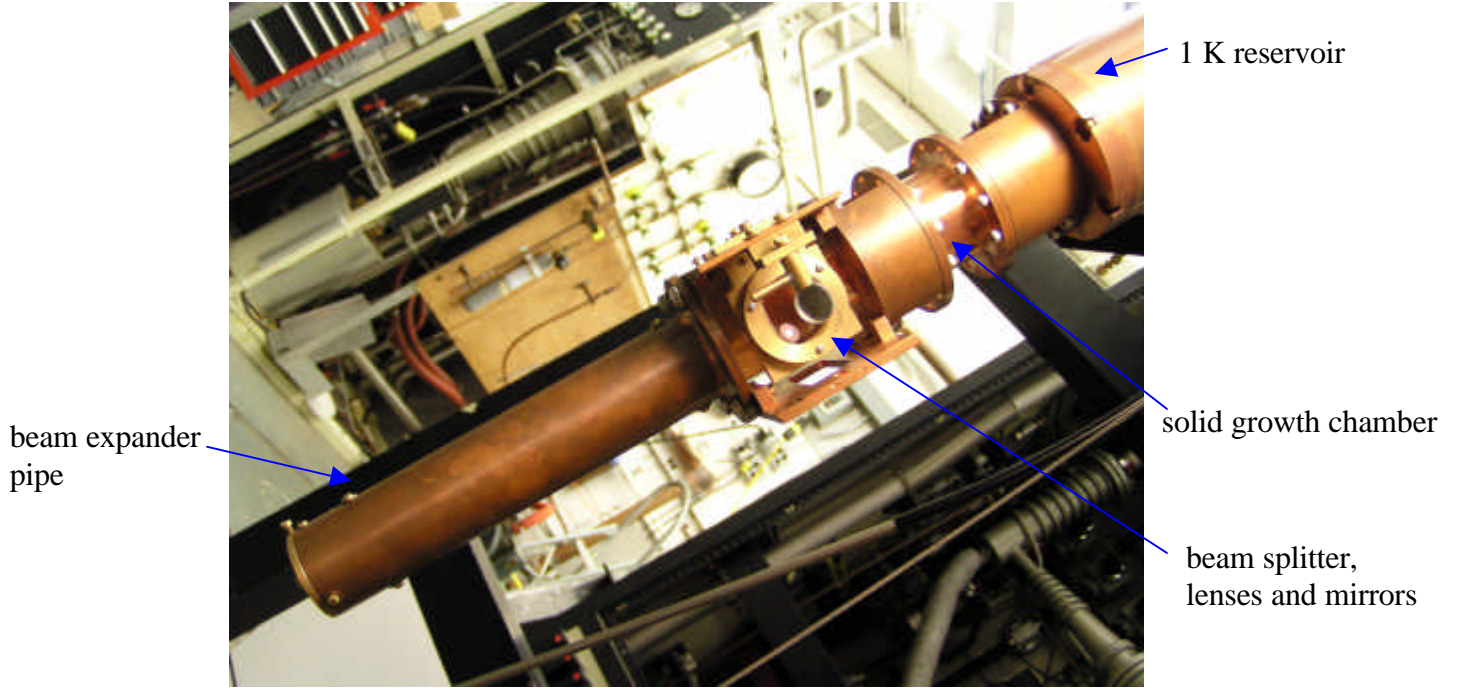


Figure 5

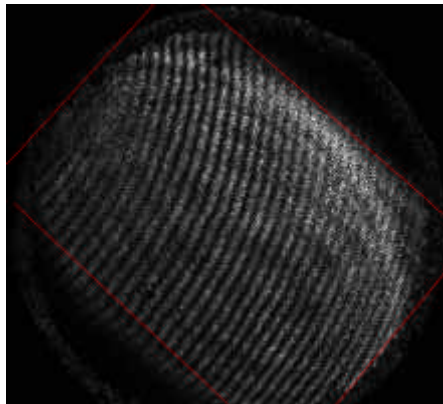
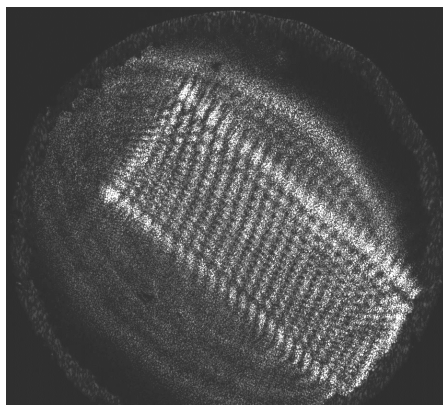


Figure 6



61
Figure 7

Acknowledgement

We have enjoyed numerous discussions with Misha Grinfeld who patiently explained to us the origin of Grinfeld instability using the pictures in Fig. 1. We wish to thank Sebastien Balibar for useful discussions. The this research is supported by NASA grant NAG3-2868.

References

* Present address: Department of Applied Physics, Tokyo Institute of Technology, Ookayama, Meguro-ku, Tokyo, Japan.

¹ M.A. Grinfeld, Dokl. Akad. Nauk. SSSR **290**, 1358(1986), (Sov. Phys. Dokl. **31**, 831(1987)).

² P. Nozieres, “*Solids Far From Equilibrium*,” ed. by C. Godereche, Cambridge University Press, 1991.

³ J. Bodenson, K. Nicolai and P. Leiderer, Z. Phys. B **64**, 55(1986).

⁴ R.H. Torii and S. Balibar, J. Low Temp. Phys. **89**, 391(1992).

⁵ H.J. Maris and T.E. Huber, J. Low Temp. Phys. **48**, 99(1982).

⁶ S. Balibar, D.O. Edwards and W.F. Saam, J. Low Temp. Phys. **82**, 119(1991).

⁷ J. Fay, W. Jian, M. Gershenson and H. Kojima, Physica **329-333**, 413(2003).

⁸ Pzt by Staveley, type EBL #2.

⁹ S. Balibar, private communication.